Stability of incoherence in an isotropic gas of oscillating neutrinos

J. Pantaleone

Department of Physics and Astronomy, University of Alaska Anchorage, Anchorage, Alaska 99508
(Received 26 January 1998; published 18 August 1998)

In the early universe and in supernovae, the flavor evolution of massive neutrinos is nonlinear. Previously, numerical simulations have explored these conditions and have sometimes found collective, synchronized neutrino oscillations. Here these coherent phenomena are studied in the simplest possible system, an isotropic gas of two-flavor neutrinos. An analytical method is used to study the stability of the incoherent state. It is found that the incoherent state has *neutral* stability. That is, a steady state synchronization can exist for all nonzero neutrino densities, but the amount depends on the initial conditions. This result is verified by numerical simulation, but it is shown that numerical simulations are accurate for only a limited time. In more complicated neutrino systems, the incoherent state could be stable or unstable. [S0556-2821(98)02919-1]

PACS number(s): 14.60.Pq

I. INTRODUCTION

There are presently several indications that the neutrino flavors are mixed by neutrino masses. Strong evidence comes from solar neutrino observations. Well tested solar models [1] calculate the rates of nuclear reactions in the Sun and, hence, also predict neutrino fluxes. These predictions require the addition of neutrino mixing in order to be compatible with the many independent observations of solar neutrinos [2]. Strong evidence for another neutrino mass comes from observations of neutrinos produced in the atmosphere by cosmic rays. The atmospheric neutrino flux ratios [3] and the angular dependence of the neutrino fluxes [4] both imply neutrino masses and mixings. In addition, measurements of neutrinos produced by a low-energy accelerator [5] suggest nonzero masses and mixing. Finally, measurements of the mass density of the universe and the structure of the universe hint at a massive neutrino (see, e.g., [6]). While it is quite likely that one or more of these latter experimental results is incorrect, the evidence for nonzero neutrino masses is quite strong.

If neutrinos have masses and mix, then neutrino flavor is not conserved, but can vary in space and time. For example, electron-neutrinos produced in the Sun can become muon- or tau-neutrinos by the time they reach the Earth. Flavor evolution between the source and the detector is used to explain all of the above experimental results. Neutrinos are unique in that their flavor evolution occurs on such large, macroscopic scales. This is because neutrino masses, which cause the flavor evolution, are so small. The experimental results suggest neutrinos masses somewhere in the range from 10^{-5} eV to 10 eV. These small values are theoretically palatable because they can emerge naturally from the structure of the standard model [7]. However they imply that neutrino mass effects may most readily be observed on astrophysical scales.

Two astrophysical environments, where the effects of a neutrino mass can be large are the early universe and supernovae. Both of these are characterized by large matter densities which trap neutrinos. This trapping allows neutrino densities to become large, which allows neutrino properties such as mass and mixing to influence directly the astrophysical environment. For example, neutrino mass effects have been related to a variety of physical phenomena in supernovae: the success of the explosion mechanism [8,9,10], r-process nucleosynthesis [11,10], and the velocity distribution of pulsars [12]. In the early universe, neutrino masses have been related to the dark matter problem (and so the formation of structure) [6], and to big bang nucleosynthesis [13]. Neutrino flavor in the early universe is relatively unconstrained, it could be much larger than the baryon asymmetry, in fact, it could even be larger than the entropy [14]. Definite statements about any of these possibilities are difficult because of the unique physical conditions present in these astrophysical phenomena, the sparsity of astrophysical observations, and the uncertainty in neutrino mass and mixing values. However there are many present and planned experiments trying to overcome these difficulties.

It is well known that the dynamics of neutrino flavor are influenced by forward scattering off of background particles. Neutrino forward scattering off of an electron background is responsible for the Mikheyev-Smirnov-Wolfenstein (MSW) effect [15] which is relevant to solar neutrino observations (for reviews, see, e.g., [9] and [16]). The large neutrino densities which make the early universe and supernovae sensitive to neutrino masses, also mean that neutrino-neutrino forward scattering occurs. When neutrinos forward scatter off of other neutrinos, they can exchange flavor coherently via the weak neutral current [17]. This nonlinear effect makes neutrino flavor dynamics a many-body phenomena. Thus, qualitatively new types of neutrino flavor evolution are possible in the early universe and in supernovae.

As detailed above, there are many ways that neutrino masses can influence supernovae and the early universe. Most studies of these possibilities simply neglect the neutrino-neutrino interaction. However there are a few exceptions, all of which have included this interaction using a density matrix approach [18,19,20]. In Ref. [21], the dynamical equations were solved perturbatively to demonstrate that the neutrino-neutrino interaction altered MSW transitions outside a supernovae's core. A subsequent numerical study of this effect found that the incoherent state provided a reasonable basis for estimating the amount of flavor evolution [22]. The incoherent state was also found to be sometimes useful for estimating flavor evolution in the early universe

[23,24]. However these latter numerical studies also observed a qualitatively new phenomenon—coherent, synchronized neutrino oscillations. It is not surprising that this new phenomena was observed in studies of the early universe and not in those of the region outside a supernovae's core. In the early universe, nonlinear dynamics dominate for a very wide range of parameters because, after electron-positron annihilation, neutrino densities are many orders of magnitude larger than all other fermion densities. Analytical descriptions of the synchronized solution have been obtained [25], in the limit of total alignment. However there has been no effort to determine if and when the incoherent state or the synchronized state is stable. This is the problem examined in this paper.

There is a sizeable literature on how collections of nonlinear oscillators become synchronized (see, e.g., [26–33] and references therein). Much of the motivation for these works comes from the many biological examples [34], such as the electrical synchrony among cardiac pacemaker cells, the chirping of crickets in unison, and the synchronous flashing in swarms of fireflies, however, there are also physical examples such as charge-density waves [35]. A particularly simple model for these phenomena was proposed by Kuramoto, which consists of a mean-field theory of coupled oscillators with an arbitrary distribution of frequencies [26]. This model has been extensively studied in the literature. It exhibits a phase transition between the incoherent state and the synchronized state. This was analytically analyzed in an notable paper by Strogatz and Mirollo [28]. As we shall see, neutrino oscillations can be rewritten in a form which is similar to the Kuramoto model. Thus, the same analytical techniques used to study collections of nonlinear oscillators can also be applied to analyze neutrino oscillations.

In this initial paper, we do not examine neutrino oscillations in either the early universe or a supernovae, but instead work with a simple, idealized system—a collection of isotropic, massive neutrinos with only two flavor degrees of freedom. In particular, we do not include a charged lepton background [15], an antineutrino background, noise [10], three flavor mixing [9], nonforward scattering or anisotropy [21]. In Sec. II the evolution equations for the neutrino density matrix are presented. We discuss how these equations are formally equivalent to those describing a collection of magnetic moments in an external field with varying intensity. They evolution equations are rewritten in a phase and angle parametrization that makes the similarity to the Kuramoto model apparent. This parametrization is also more intuitive and allows us to identify easily the complex order parameter of the system. In Sec. III we discretize the evolution equations and numerically study the behavior of the order parameter. The limitations on numerical methods are also discussed. In Sec. IV we define a single, governing density function. The evolution equation describing this is linearized, and solved analytically. In Sec. V, we summarize our results and discuss their implications. An appendix contains details of the calculation.

II. THE FLAVOR EVOLUTION EQUATIONS

Our goal is to describe the flavor evolution of a dilute, multi-neutrino gas. The initial assumption is the Hartree approximation—that each neutrino in the gas is described by its own wave function and is subject to an equivalent potential due to the other neutrinos. The Pauli blocking and other such fermion symmetry effects are neglected, so only dilute systems are considered. For these initial inquiries, some further approximations are made to simplify the physical situation. It is assumed that there are only two neutrino flavors, that the neutrino gas is uniform and isotropic, and that the physical system does not contain charged leptons or antineutrinos. Under all these assumptions, the flavor dynamics can be easily formulated.

We choose to work with bilinears of the neutrino wave function because that is what the neutrino-neutrino potential depends on. In the flavor basis, the one particle density matrix is

$$\rho_F(i;t,k) = \begin{bmatrix} \rho_{ee} & \rho_{e\mu} \\ \rho_{\mu e} & \rho_{\mu\mu} \end{bmatrix}_i = \begin{bmatrix} \nu_e \\ \nu_\mu \end{bmatrix} [\nu_e^* \quad \nu_\mu^*]_i(t,k). \quad (1)$$

Here ν_α is the slowly varying part of the ith neutrino's wave function of flavor α with energy/momentum k at time t. Neutrinos are created and destroyed in the flavor basis, but the vacuum mass eigenstate basis is more convenient for the dynamics. The vacuum mass matrix take the simplest form when written in the vacuum mass eigenstate basis, ρ_V.

$$\rho_V(i;t,k) = U^\dagger \rho_F(i;t,k) U \quad (2)$$

$$\begin{bmatrix} \rho_{11} & \rho_{12} \\ \rho_{21} & \rho_{22} \end{bmatrix} = \begin{bmatrix} C_\theta & -S_\theta \\ S_\theta & C_\theta \end{bmatrix}$$

$$\times \begin{bmatrix} \rho_{ee} & \rho_{e\mu} \\ \rho_{\mu e} & \rho_{\mu\mu} \end{bmatrix}_i \begin{bmatrix} C_\theta & S_\theta \\ -S_\theta & C_\theta \end{bmatrix}. \quad (3)$$

Here U is the (time independent) vacuum mixing matrix which rotates from the flavor basis to the vacuum mass eigenstate basis with $C_\theta = \cos\theta$ and $S_\theta = \sin\theta$ (the notation is consistent with the conventions in Ref. [9]). The coupled, nonlinear equations [23,20,21] describing the temporal flavor dynamics are

$$i\frac{\partial}{\partial t}\rho(i;t,k) = [V(t,k;\rho), \rho(i;t,k)]. \quad (4)$$

In the vacuum mass eigenstate basis, the effective potential, V, takes the form:

$$V_V(t,k;\rho_V) = \frac{\Delta}{4k}\begin{bmatrix} -1 & 0 \\ 0 & 1 \end{bmatrix} + \sqrt{2}G_F \int \frac{d^3\vec{q}}{(2\pi)^3}\sum_j \rho_V(j;t,q)$$

$$(5)$$

here $\Delta = m_2^2 - m_1^2$ is the difference in neutrino vacuum masses squared, G_F denotes Fermi's constant and k is the neutrino momentum. The first term in the potential describes the effects of the vacuum mass parameters. The second term comes from neutrino forward scattering off of background neutrinos via the weak neutral current. This potential depends on the sum over all neutrinos in the background. One neutrino couples equally to all of the other neutrinos in the

system because of the assumption that our gas is isotropic and uniform (in an anisotropic system, there are additional effects [21]). The neutrino-neutrino forward scattering potential contains flavor diagonal [36] and flavor off-diagonal [17] contributions. Note that the evolution equations do not depend on the vacuum mixing angle, θ. The vacuum mixing angle enters the dynamics only through the initial conditions.

The potential in the dynamical equations only depends on the neutrino momentum and the total neutrino density matrix. Thus, the evolution equation is the same for all neutrinos with the same momentum. Hence, the equations also apply to sums of the one-particle density matrix over neutrinos with the same momentum.

$$\rho(t,k)=\sum_i \rho(i;t,k). \tag{6}$$

A. Angle-phase parametrization

The elements of the density matrix have straightforward physical interpretations. However the density matrix formalism is generally not the best to use for studying the dynamics. It is very inefficient, since there are fewer free parameters than their are elements of the density matrix. Here we choose to reparametrize the neutrino evolution dynamics in terms of an effective mixing angle, $\theta(t,k)$, and oscillation phase, $\phi(t,k)$. Similar parametrizations have been used to study how a charged lepton background affects the oscillations of a neutrino (see, e.g., [9] and references therein). Specifically, the density matrix elements can be parametrized as

$$\frac{\rho_{22}(t,k)-\rho_{11}(t,k)}{2}=D(k)\cos[2\,\theta(t,k)]$$

$$\rho_{12}(t,k)=-D(k)\sin[2\,\theta(t,k)]\exp[i\,\phi(t,k)]. \tag{7}$$

The mixing angle lies in the range $(\pi/2)>\theta(t,k)>0$, while there are no restrictions on $\phi(t,k)$. This parametrization is designed to incorporate all of the general constraints on density matrix elements. The diagonal elements are real because the density matrix is Hermitian. The trace of the density matrix is the total neutrino density and it is a conserved quantity. It drops out of the evolution equations, so we need only to parameterize the difference of the diagonal elements, which is the flavor asymmetry in the neutrino background. The trace of the square of the density matrix is proportional to the total entropy of the system [18] and is a conserved quantity because we have neglected dissipative effects like nonforward scattering. This constraint forces the magnitude squared of the elements in Eqs. (7) to be time independent, and that magnitude is denoted here by $D(k)$.

Because this parameterization satisfies all of the general constraints on a neutrino density matrix, we could use it to describe either the one-particle matrices, $\rho(i;t,k)$, or the multi-neutrino density matrices of Eq. (6), $\rho(t,k)$. The interpretation of the elements of the parametrization is different for these different cases. For a one particle density matrix,

$D(k)$ is just one per unit volume. For the multi-neutrino density matrix, cancellations typically occur in the summation between neutrinos with different phases and different mixing angles, and so then $D(k)$ is much smaller than the total neutrino density with momentum k. For this paper we adopt an intermediate approach. We apply the parameterization of Eq. (7) to density matrices which are a sum of identical one-particle density matrices of both ''species.'' Specifically, the sum is over all ''neutrinos'' with momentum k, phase $\phi(t,k)$ and mixing angle $\theta(t,k)$ plus those with phase $(\phi(t,k)+\pi)$ and mixing angle $(\pi-2\,\theta(t,k))$. In the summation, complete cancellation occurs between one-particle density matrices of these two ''species.'' To fix the ambiguity in the resultant mixing angle, we additionally require that $D(k)$ is always nonnegative (which will be important in Sec. IV). If all neutrinos happen to have the same phase and mixing angle at some time, then we can identify $D(k)$ as the total flavor asymmetry per unit volume, but otherwise it is smaller than that. In the potential, the total neutrino density matrix is relevant so there is still an additional summation there over different phases, mixing angles and momentum. In the notation adopted here, this summation over phases and mixing angles will be denoted by a discrete summation sign, but we shall henceforth drop the indices labeling different phase and mixing angles with the same momentum.

It is actually slightly more convenient to use the parameter ω instead of the momentum parameter k.

$$\omega=\frac{\Delta}{2k}. \tag{8}$$

ω is the vacuum oscillation frequency and is inversely proportional to the neutrino momentum, k. The evolution equations can then be rewritten in the angle-phase parametrization as

$$\frac{\partial\theta(t,\omega)}{\partial t}=-\frac{\xi}{2}\tan(2\,\theta_F)R(t)\sin[\phi(t,\omega)-\psi(t)]$$

$$\frac{\partial\phi(t,\omega)}{\partial t}=\omega+\xi-\xi\tan(2\,\theta_F)\cot[2\,\theta(t,\omega)]$$

$$\times R(t)\cos[\phi(t,\omega)-\psi(t)]. \tag{9}$$

The neutrino-neutrino forward scattering potential depends on the sum over all neutrinos in the background and this enters the dynamics in the parameters θ_F, ξ and R.

Here θ_F is the average mixing angle, defined as

$$\cos(2\,\theta_F)=\int\frac{d\mathcal{N}_\omega}{\mathcal{N}_\omega}\frac{1}{N_d}\sum\cos[2\,\theta(t,\omega)] \tag{10}$$

where N_d is the total number of terms in the discrete sum and $\mathcal{N}_\omega$ is the total of the continuous sum over the neutrino asymmetry distribution

$$d\mathcal{N}_\omega=\frac{k^2}{2\,\pi^2}D(k)dk. \tag{11}$$

Although it is not apparent from its definition, θ_F is time-independent: it is specified by the initial conditions. This conserved quantity follows because neutrino-neutrino forward scattering, and so all of the evolution equations respect L_1 and L_2, the lepton number family symmetries [17]. A charged lepton background would break this symmetry and then θ_F would be time dependent. The parameter ξ is just proportional to $\cos(2\theta_F)$, and so it too is time independent

$$\xi = 2\sqrt{2} G_F \cos(2\theta_F) \mathcal{N}_\omega N_d \tag{12}$$

where $\mathcal{N}_\omega N_d$ is the total neutrino asymmetry per unit volume. ξ is the neutrino-neutrino forward scattering induced potential—it is similar to the parameter used in calculations of the MSW effect [15], $A/k = 2\sqrt{2} G_F N_e$, where N_e is the electron density. The neutrino-neutrino potential depends only on the net flavor asymmetry in the neutrino background as measured by $\cos(2\theta_F)$. Independent of where it comes from, ξ acts as a coupling between the different oscillators. All nonlinear effects enter through the ξ coupling constant.

The remaining expression in the dynamical equations, Eqs. (9), is a complex order parameter

$$R(t)\exp[i\psi(t)] = \frac{1}{\sin(2\theta_F)} \int \frac{d\mathcal{N}_\omega}{\mathcal{N}_\omega} \frac{1}{N_d}$$

$$\times \sum \sin[2\theta(t,\omega)]\exp[i\phi(t,\omega)]. \tag{13}$$

This order parameter measures the degree of coherence in the system. If the neutrino oscillations are incoherent, then R=0, while if the neutrinos are completely synchronized, then R=1. All of the dynamics depend on this single order parameter.

In the limit where the total neutrino background asymmetry density vanishes, ξ vanishes and the situation reduces to purely vacuum oscillations. Then the dynamical equations, Eqs. (9), tell us that the mixing angle, $\theta(t,\omega)$, is a constant and that the phase evolves linearly with frequency ω. For neutrinos created at t=0 in the flavor eigenstates, the mixing angle is just the vacuum angle $\theta(t,\omega) = \theta$, the phase will be $\phi(t,\omega) = \omega t$, and $D(k) = [\rho_{22}(0,k) - \rho_{11}(0,k)]/2 \cos(2\theta)$.

For the physical environments of the early universe or a supernovae, the neutrinos started off in thermal equilibrium. Flavor asymmetries can be present in equilibrium as chemical potentials, or they may be generated as the neutrinos leave equilibrium, but regardless, the neutrinos are expected to retain an approximately thermal distribution. Thus $D(k)$ is typically roughly proportional to a Boltzmann factor, and so the neutrino asymmetry distribution, Eq. (11), is expected to vanish exponentially at large momentum. At small momentum the neutrino asymmetry distribution vanishes because of phase space factors. In terms of frequency, a physical neutrino asymmetry distribution is nonzero over all $\omega > 0$, but falls off very quickly at each end of its range. Here we parameterize the frequency distribution as
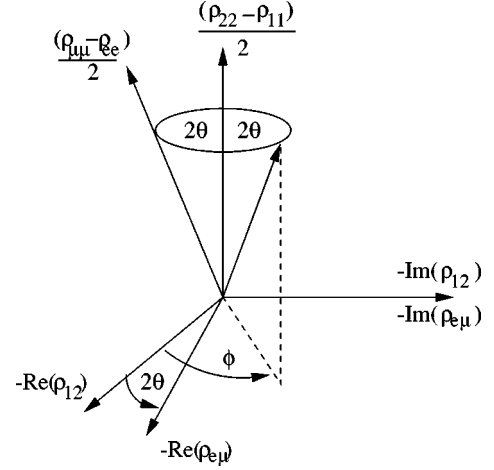

FIG. 1. A graphical representation of neutrino evolution in terms of the phase and mixing angle parameterization.

$$\frac{d\mathcal{N}_\omega}{\mathcal{N}_\omega} = g(\omega) d\omega \tag{14}$$

where $g(\omega)$ is normalized to one per unit volume. Note that $g(\omega)$ can always be chosen to have a mean of zero. That is, we can redefine the phase $\phi(t,\omega)$ by going to a rotating reference frame so that the frequency distribution has a mean at zero frequency (e.g., $\omega \rightarrow \omega + \bar{\omega}$, $\phi \rightarrow \phi + \bar{\omega}t$). Then the average frequency, $\bar{\omega}$, drops out of the dynamical equations. Thus, the flavor dynamics do not depend on the average vacuum frequency, but do depend on the width of the frequency range, and how these frequencies are distributed. Also note that it follows from our previous convention of a nonnegative $D(k)$ that $g(\omega)$ is always nonnegative.

B. Graphical representation

The angle-phase parametrization allows an instructive graphical representation. The details of the graphical representation are not unique. Different choices in sign conventions, or using wave functions instead of density matrices, lead to different representations (see, e.g., [16]). For the conventions assumed here, Fig. 1 shows the graphical representation. The flavor basis and the vacuum mass eigenstate basis are represented by three dimensional coordinate systems which coincide along the $\text{Im}(\rho_{12}) = \text{Im}(\rho_{e\mu})$ axis. The other axes differ in direction by a relative rotation angle of 2θ. The neutrino density matrix (as defined here) is represented as a single vector of length D at a zenith angle of 2θ and a tangential angle of ϕ. Vacuum oscillations correspond to precession of this vector about the vacuum eigenstate axis at a zenith angle of 2θ. The neutrino dynamics we are considering depend on the average properties of the entire neutrino population. The time independent parameter $\cos(2\theta_F)$ corresponds to the average vector component along the vacuum mass eigenstate direction. The average vector components in the directions perpendicular to this axis correspond to the real and imaginary parts of the order parameter, $R \exp(i\psi)$. An incoherent population of vacuum neutrinos can be represented by a collection of vectors uniformly distributed along

a cone at a zenith angle of 2θ about the vacuum mass eigenstate direction. Such an incoherent population has a vanishing order parameter.

C. Magnetic moments analogy

Many authors have used the analogy between neutrino oscillations and the motion of a spin in a magnetic field. This analogy continues to hold when the flavor evolution is influenced by neutrino-neutrino forward scattering. It is useful to make this connection explicit.

Consider a collection of magnetic moments with angular momentum $\vec{L}_i$ and magnetic moment $\vec{\mu}_i = \mu_B \vec{L}_i$. The magnetic moments are in an external magnetic field which is everywhere parallel, but the intensity of which varies among the magnetic moments $\vec{B}_i$. The total magnetic field felt by any magnetic moment depends on the external magnetic field and also on that produced by the magnetic moments. With the assumption that all magnetic moments contribute equally, then the total magnetic field is $\vec{H}_i = \vec{B}_i + \zeta \Sigma \vec{\mu}_j$, where ζ is a coupling parameter. Then the equation of motion of the ith magnetic moment is given by $d\vec{L}_i/dt = \mu_B \vec{L}_i \times \vec{H}_i$. We choose the direction of the external magnetic field $\vec{B}_i$ to be the z direction, and parameterize the angular momentum in the usual spherical coordinates, but with a zenith angle twice the conventional definition $\vec{L}_i = L(\sin 2\theta_i \cos \phi_i, \sin 2\theta_i \sin \phi_i, \cos 2\theta_i)$. Then the equations of motion can be written as

$$\frac{\partial \theta_i}{\partial t} = -\frac{\zeta}{2}\mu_B^2 L \sum_j \sin(2\theta_j)\sin(\phi_j - \phi_i)$$

$$\frac{\partial \phi_i}{\partial t} = -\mu_B B_i - \zeta \mu_B^2 L$$

$$\times \left(\sum_j \cos(2\theta_j) - \cot(2\theta_i) \right.$$

$$\left. \times \sum_j \sin(2\theta_j)\cos(\phi_j - \phi_i) \right). \quad (15)$$

These equations of motion are a completely discrete version of those given in Eq. (9) describing neutrino flavor dynamics. When the moment-moment coupling vanishes, the spins just precess around the external field at a constant zenith angle with the frequency $\omega = -\mu_B B_i$. The $\Sigma_j \cos(2\theta_j)$ is time-independent because the total angular momentum in the direction of the external magnetic field is conserved. The order parameter is the average magnetic field in the x and y directions, $(1/n)\Sigma_j \sin(2\theta_j)\exp(i\phi_j) \propto \langle H_x + iH_y \rangle$ and it is the same for all magnetic moments.

Similar models have been studied to try to understand how oscillators become synchronized.

D. Kuramoto model

Kuramoto proposed an analytically tractable model for studying the collective synchronization of oscillators [26].

This model was not derived from any specific physical system, but was intended to model the essential behavior of biological systems [37]. It can be ''motivated'' from a magnetic moments approach with a couple of additional assumptions beyond those used in the previous section. The zenith angle degree of freedom is removed by restricting all magnetic moments to have the same zenith angle, so the Kuramoto model is like an X-Y model [31]. Also a source of dissipation must be added.

The equations of motion for the Kuramoto model are

$$\frac{\partial \phi_i}{\partial t} = \omega_i - \frac{K}{N}\sum_{j=1}^{N} \sin(\phi_i - \phi_j) \quad (16)$$

where K is a coupling constant and i ranges from 1 to N. Introducing the order parameter

$$re^{i\psi} = \frac{1}{N}\sum_{j=1}^{N} e^{i\phi_j}. \quad (17)$$

Then the equations of motions may be rewritten as

$$\frac{\partial \phi_i}{\partial t} = \omega_i - Kr \sin(\phi_i - \psi). \quad (18)$$

This model has been studied extensively [28–33]. For $K > 0$ and large N, it has been shown that there is a critical value for the coupling constant

$$K_c = \frac{2}{\pi g(0)}. \quad (19)$$

Here $g(\omega)$ is the density of oscillators, assumed to be symmetric about and peaked at the mean frequency, zero [see, e.g., Eq. (14)]. For K less than K_c, the incoherent state was found to have ''neutral'' stability, with synchronization decaying at a rate which is exponential at intermediate times, but which is slower than exponential at long times. This decay mechanism is similar to Landau damping of waves in a collisionless plasmas [30]. For K above K_c, the incoherent state is always unstable and spontaneous synchronization of the oscillators occurs. Then, when the order parameter is small it grows like $R(t) \approx R_0 e^{\lambda t}$. The growth parameter, λ, is determined by [28]

$$1 = \frac{K}{2}\int_{-\infty}^{\infty} d\nu \frac{g(\nu)}{\lambda + i\nu}. \quad (20)$$

Thus there is a phases transition in the system as the coupling parameter, K, is varied.

It is apparent that the evolution equations of the Kuramoto model, Eqs. (18) and (17), are quite similar to those describing the flavor evolution of a dilute neutrino gas, Eqs. (9) and (13). The parameter K in the Kuramoto model is analogous to the parameter ξ in the neutrino gas model. The fact that the neutrino flavor evolution depends on two parameters is not that important because it is the evolution of the phase, ϕ which is most crucial to synchronization. The largest difference between neutrino flavor evolution and the

Kuramoto model is that the former depends on a cosine coupling of the phases, while the latter depends on a sine coupling. There has only been minimal attention in the synchronization literature to nonlinear couplings other than a sine [27]. With a cosine coupling, some methods used to study the Kuramoto model are not practical. For example, it is difficult to find a Lyapunov function [31]. However the method used by Strogatz and Mirollo [28] to determine the stability of the incoherent state, and to calculate analytically the rate of growth of the synchronized state, is still applicable. This method will be used in Sec. VI to study the dilute neutrino gas.

III. THE DISCRETE MODEL AND ITS NUMERICAL ANALYSIS

The neutrino evolution equations, Eqs. (9), were studied numerically. This was done in order to understand the behavior of the system, to verify the results of analytical calculations, and to look for unexpected behavior. For the numerical calculations, the frequency, ω, was divided into N_ω uniform bins, turning the integral over frequency into a discrete sum. Then each ''neutrino'' had a particular frequency. The number of ''neutrinos'' with the same frequency is given by N_d. A fourth order Runge-Kutta method was used to evolve the angle and phase parameters for each ''neutrino.''

A. Numerical errors

There are two places where numerical errors can manifest themselves, in the discrete approximation to the derivatives with respect to time or the discrete approximation to the integral over frequency. Each source of error is important and cannot be ignored.

It is straightforward how to achieve accuracy using the Runge-Kutta approximation. For the numerical results given here, the time step was chosen to be a couple orders of magnitude smaller than the largest frequency. The efficacy of this choice was tested by two different techniques. One check was provided by the average mixing angle, $\cos(2\theta_F)$. While the mixing angle of a typical ''neutrino'' changed considerably in time, the average mixing angle should remain constant [see, e.g., Eq. (10)]. A different check was provided by the constraint that the mixing angle for each ''neutrino'' should always stay in the range $0 < \theta < \pi/2$. These constraints were tested at each time step, and violations of them were eliminated by restarting the calculation with a smaller time steps.

Making the frequency discrete produces errors that are more difficult to monitor. The problem can be illustrated with a sample calculation. Here we calculate the order parameter, Eq. (13), exactly for the continuous case and for a discrete approximation. This can be done when the nonlinear effects are negligible ($\xi=0$), so only vacuum oscillations are relevant. We look at the simplest possible case, a uniform frequency distribution

$$g(\omega) = \begin{cases} \dfrac{1}{2\gamma} & \text{for } -\gamma < \omega < \gamma, \\ 0 & \text{otherwise.} \end{cases} \quad (21)$$

It is assumed that the ''neutrinos'' are completely synchronized at t=0, i.e., they all have the same mixing angle and zero phase, so $R(0)=1$. There is no evolution of the mixing angle in the vacuum case, so it drops out of the expression for the order parameter. Then integration yields $\psi=0$ and

$$R(t) = \frac{\sin(\gamma t)}{\gamma t}. \quad (22)$$

The order parameter decreases in time and slowly approaches zero, showing that vacuum oscillations slowly disappear and the neutrinos become incoherent. To calculate the discrete version, we choose the parametrization $\omega_j = \gamma[-1+2j/(N_\omega+1)]$ where j runs from 1 to N_ω. Then summing the series yields $\psi=0$ and

$$R(t) = \frac{\sin[(\gamma t)N_\omega/N_\omega+1]}{N_\omega \sin[(\gamma t)1/N_\omega+1]}. \quad (23)$$

The discrete expression for R initially decreases, in agreement with the continuous case. But subsequently, the discrete expression increases, and in fact it periodically returns to 1, an example of Poincare recurrence. The continuous and discrete expression agree when N_ω is large compared to 1 and, more importantly, when the total time is small such that

$$\gamma t \approx 2\pi n_{osc} \ll N_\omega. \quad (24)$$

Here n_{osc} is the number of oscillations that the order parameter has gone through. Thus the number of frequency bins, N_ω places an upper limit on how long we can evolve the equations and still trust the numerical results to agree with the continuous model.

B. Evolution of volumes in phase space

The relation Eq. (24) was derived for vacuum oscillations, but it should still roughly hold when the nonlinear terms are small compared to the vacuum terms. However when the nonlinear terms are large, the situation can be very different. *A priori*, it is possible that then phenomena such as Poincare recurrence occur leading to huge errors, or perhaps there are attractors and the errors are vanishing. These possibilities can be explored somewhat by examining how volumes in phase space evolve for the discrete model. For example, volumes in the Kuramoto model's 2N dimensional phase space obey

$$\frac{1}{V}\frac{dV}{dt} = \sum_{i=1}^{N} \frac{\partial}{\partial \phi_i} \dot{\phi}_i \quad (25)$$

$$= -K(Nr^2 - 1). \quad (26)$$

Here r is the order parameter, Eq. (17). This equation tells us that, for large N, a small amount of coherence cause volumes in phase space to shrink, suggesting the presence of an attractor. This qualitative observation agrees with experience from numerical simulations of the Kuramoto model, where it is found that the steady state value of the order parameter is

insensitive to the initial conditions. For the neutrino model, volumes in the 4N dimension phase space obey

$$\frac{1}{V}\frac{dV}{dt} = \sum_{i=1}^{N}\left(\frac{\partial}{\partial\phi_i}\dot{\phi}_i + \frac{\partial}{\partial\theta_i}\dot{\theta}_i\right) \tag{27}$$

$$= \xi N R S \sin(\chi - \psi), \tag{28}$$

where R is the discretized version of the order parameter defined in Eq. (13), and S is an analogous quantity

$$S e^{i\chi} = \frac{1}{N}\sum_{j=1}^{N}\frac{\cot(2\theta_j)}{\cot(2\theta_F)}e^{i\phi_j}. \tag{29}$$

When all neutrinos have the same mixing angle, S and R are identical, so Eq. (28) vanishes and the system is conservative—volumes in phase space are preserved. In general, the mixing angle will have a distribution of values (from MSW type effects), so S and R are typically different and the system is not always conservative. However, it naively appears that Eq. (28) will typically oscillate in sign, and so the neutrino system is approximately conservative on the average. This suggests that there is no robust attractor for the discrete neutrino model. Consequently, it should be expected that, for all values of the nonlinear coupling, numerical simulations of the neutrino model will depend on initial conditions, and the discrete and continuous models will diverge with time, analogous to Eq. (24).

C. Numerical results

The general numerical strategy employed here is to always choose parameters for the total evolution time and the number of bins that satisfy Eq. (24). In addition, the time evolution of the order parameter is always monitored for large fluctuations, and compared to a recalculation with a different number of frequency bins. This is an improvement over all previous numerical studies of neutrino-neutrino flavor dynamics which have neglected the difference between the continuous and discrete models. Some previously published numerical studies have evolved neutrino systems for far longer than the limit given in Eq. (24). Thus numerical results on nonlinear neutrino dynamics in the existing literature must be used with caution.

Our numerical solutions of the neutrino dynamics model, Eqs. (9), are given in Figs. 2–4. These solutions are for a uniform neutrino asymmetry distribution, as given in Eq. (21). The parameter which sets the scale for vacuum oscillations, γ, was chosen to be 1. The "neutrinos" were always started with a common mixing angle, $(\theta(0,\omega) = \theta_F)$, but several values of θ_F were used. While these are not the most general conditions, they are adequate for illustrating the type of behavior that occurs in neutrino dynamics.

Two different types of initial conditions were used for the phase, $\phi(t,\omega)$. Sometimes the "neutrinos" were started completely synchronized with $N_d = 1$ and $\phi(0,\omega) = 0$ so that $R(0) = 1$. The other initial condition used was to start with incoherent "neutrinos", i.e., the phases of the N_d "neutrinos" that have the same frequency were started out uni-
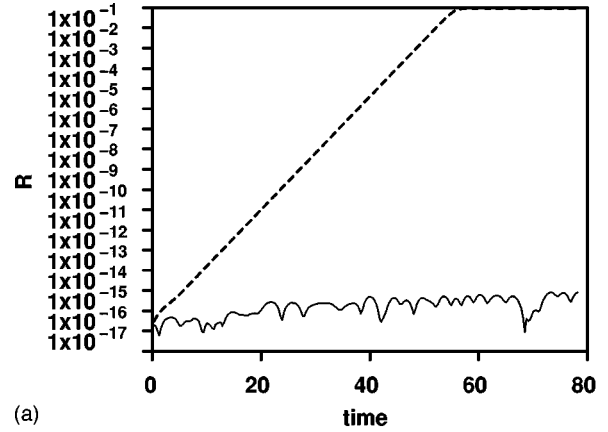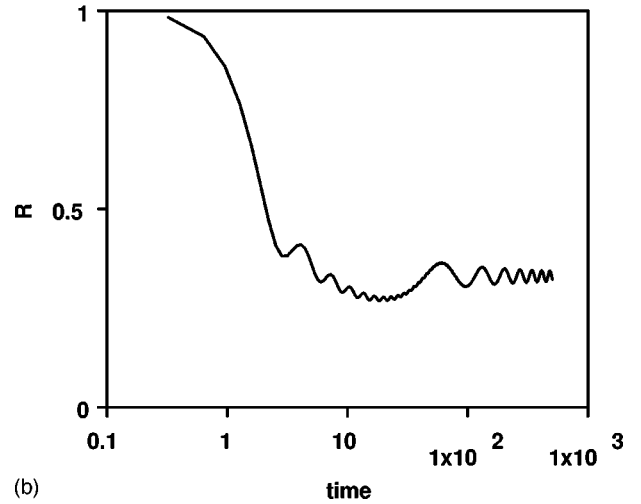
FIG. 2. Plots of the magnitude of the order parameter as a function of time. In (a) the $N_\omega = 300$, $N_d = 10$ "neutrinos" were initially incoherent $[R(0) = 0]$, with $\xi = 2.0$ and $\theta_F = 0.25$. For comparison, the dashed line in (a) shows the behavior of the Kuramoto model for $K = 2.0$. In (b) the $N_\omega = 2000$, $N_d = 1$ "neutrinos" were initially synchronized $[R(0) = 1]$, with $\xi = 0.5$ and $\theta_F = 0.25$.

formly distributed between 0 and 2π so that $R(0) = 0$. The latter was useful for studying the growth of coherence.

Figures 2 show the evolution of the magnitude of the order parameter. The behavior of the "neutrinos" for a large value of the neutrino background coupling and incoherent initial conditions is illustrated in Fig. 2(a). Initially $R(0) = 0$, but subsequently, the finite precision of machine calculations introduces small amounts of noise to this quantity. In the Kuramoto model (dashed line), the order parameter grows exponentially, from these small fluctuations to a completely synchronized steady state. However for the model of neutrino dynamics studied here, the fluctuations in the order parameter do not grow exponentially, but instead appear to remain consistent with numerical zero. Calculations at other values of ξ show the same behavior, neutrinos which are initially incoherent remain incoherent. For the Kuramoto model, the incoherent state is unstable, but this is not so for the neutrino model. However this does not mean that the incoherent state is stable for neutrinos. In Fig. 2(b) the "neutrinos" are started off completely coherent, with only a small value for the neutrino background coupling, ξ. Initially
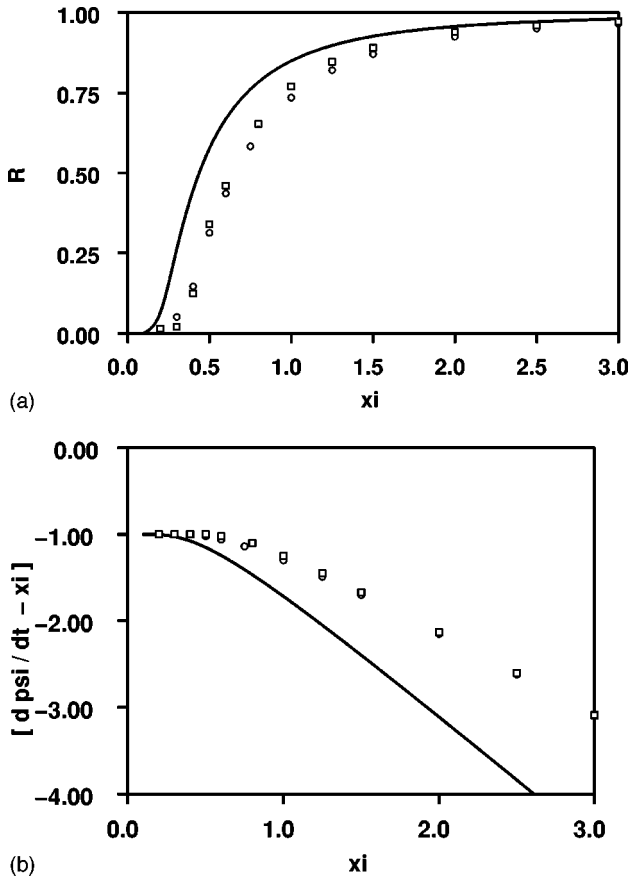
(a)

(b)

FIG. 3. Plots of steady state values of the order parameter's magnitude (a) and rate of phase change (b) as a function of ξ, the neutrino background density parameter. The ''neutrinos'' were initially synchronized $[R(0)=1]$, and two different values of initial mixing angle were used, $\theta_F=0.125$ (circles) and $\theta_F=0.25$ (squares). The solid curves denote approximate analytical calculations.

$R(0)=1$, but subsequently, the order parameter decreases, undergoes large and small scale oscillations, and ultimately settles down to a nonzero steady state value. Because the order parameter settles down to a nonzero value, we know that the incoherent state is not an attractive, stable state, even at small ξ. This is different than the Kuramoto model (not plotted), where the order parameter relaxes completely to zero below the critical coupling, Eq. (19). These results clearly show that the neutrino steady state is sensitive to the initial conditions, as expected from Eq. (28). In general, it appears that the nonlinear neutrino dynamics in this simple model does not cause synchronization to increase, but does support some synchronization, even when the neutrino background is small.

The amount of steady state synchronization that remains when starting from initially coherent neutrinos is explored in Fig. 3. There the steady state values of the order parameter's magnitude (a) and rate of phase change (b) are plotted as a function of the coupling, ξ, for two different values of the mixing angle, θ_F. Also shown on these figures are the approximate theoretical predictions from Eq. (A9). Only positive ξ values are shown in these figures because, for even
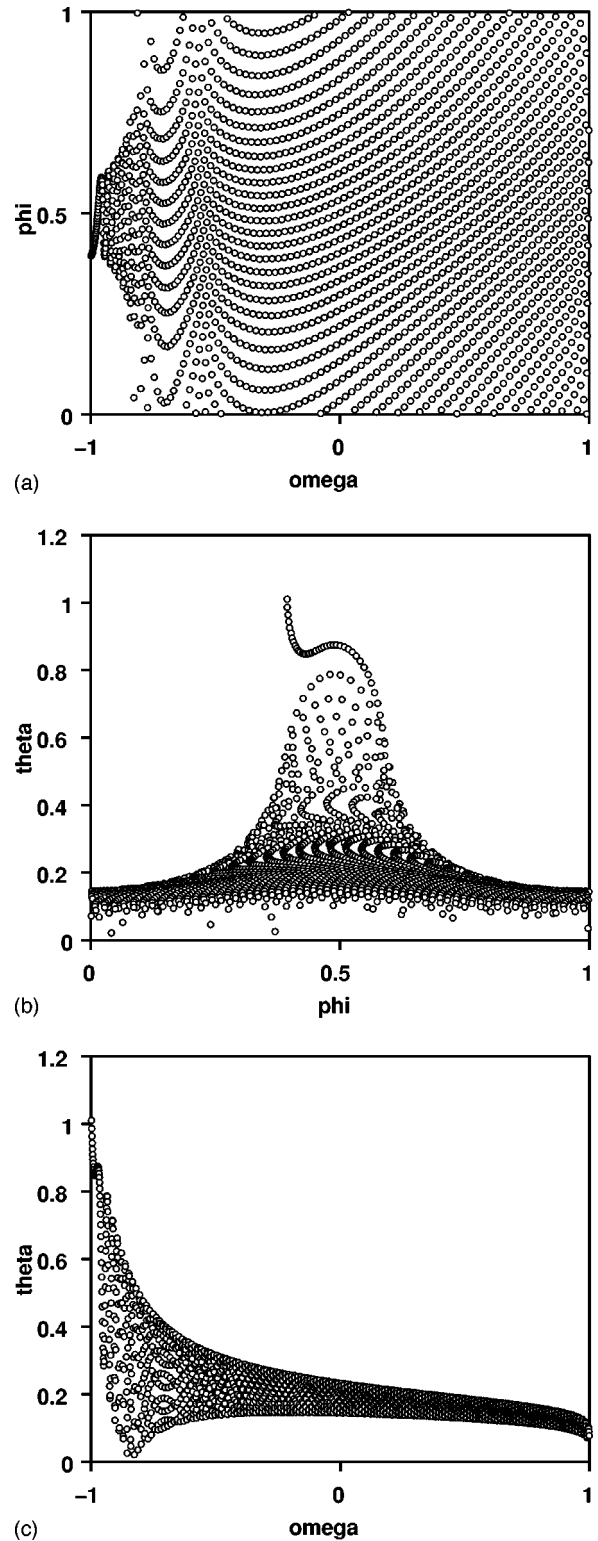

(a)

(b)

(c)

FIG. 4. Plots of the steady state values of $N_\omega=2000$, $N_d=1$ oscillators. The ''neutrinos'' were initially synchronized $[R(0)=1]$, with $\xi=0.5$ and $\theta_F=0.25$. Figure (a) shows the phase versus the frequency, figure (b) shows the mixing angle versus the phase, and figure (c) shows the mixing angle versus the frequency. The phase in these figures has been binned and scaled to range from 0 to 1.

$g(\omega)$, R is an even function of ξ, while ψ is odd. The magnitude of the order parameter approaches 1 for large ξ, but decreases towards 0 as ξ decrease. The phase of the order parameter changes at a constant, nonzero rate in the steady state. This is shown in Fig. 3(b) which plots $(d\psi/dt - \xi)$ versus ξ. Note that it is difficult to calculate numerically the steady state value of the order parameter and its phase when ξ is small. This is because then the order parameter initially falls off approximately as given in Eqs. (22) and (23), which is rather slow, so very long calculations times are needed [see Eq. (24)] to discern the small, residual synchronization. In general, there does not appear to be a sharp change in the order parameter at any nonzero value of ξ.

The distribution of ''neutrinos'' in the steady state is explored in Fig. (4). There are plotted the state of each oscillator at the end of the evolution shown in Fig. 2(b). These plots are for initially synchronized neutrinos with a relatively small value of the coupling, ξ. Figure 4(a) shows the distribution of the neutrino phases as a function of frequency. The phases have had multiples of 2π subtracted off, and their remainder scaled to range from 0 to 1. This figure shows that the phase grows continuously with frequency. Figure 4(b) plots the mixing angle of each ''neutrino'' versus its phase. Crudely, this figure shows a ''background'' of continuously distributed ''neutrinos'' and a rather localized structure corresponding to the synchronized neutrinos. Note that the phase associated with the center of the localized structure in Fig. 4(b) changes in time, as illustrated in Fig. 3(b). Figure 4(c) plots the mixing angle of each ''neutrino'' versus its frequency. The mixing angle in Figs. 4(b) and 4(c) has not been scaled and can range from 0 to $\pi/2$. While the average of the mixing angles must remain equal to their initial value, $\theta_F = 0.25$, these figures show considerable structure. The steady state mixing angle is a function of frequency, has small scale oscillations and also large scale distortions.

The plots shown in Fig. 4 would appear quite different if calculated for large values of the coupling ξ. At large coupling, the continuous background in Fig. 4(c) disappears and all of the neutrinos are in a localized structure. Thus, there is a transition from partial entrainment to full entrainment. However Fig. 3 indicates that the order parameter is continuous and nonzero as ξ is varied through this transition.

IV. ANALYTICAL SOLUTIONS

The stability of the incoherent state of the continuous neutrino model can be analyzed analytically. The methods used here are similar to those used in studies of the Kuramoto model [28] and in studies of two component limit cycle oscillators [29]. The first step is to introduce a density function $\rho(\tilde{\theta}, \phi, \omega, t)$. Here the parameter $\tilde{\theta} \equiv 2\theta$ is used since $\tilde{\theta}$ and ϕ follow the usual rules for spherical coordinates. This density function is the fraction of the oscillators of frequency ω between $\tilde{\theta}$ and $\tilde{\theta} + d\tilde{\theta}$ and between ϕ and $\phi + d\phi$. It obeys the normalization condition

$$\int_0^\pi d\tilde{\theta} \sin(\tilde{\theta}) \int_0^{2\pi} d\phi \rho(\tilde{\theta}, \phi, \omega, t) = 1 \qquad (30)$$

for all t and ω. This density function should not be confused with the neutrino density matrix. The density function is a single quantity which describes how the elements of the density matrix are distributed.

The evolution equation for $\rho(\tilde{\theta}, \phi, \omega, t)$ is just the equation for conservation of oscillators:

$$\frac{\partial \rho}{\partial t} + \boldsymbol{\nabla} \cdot (\rho \mathbf{v}) = 0 \qquad (31)$$

where $\mathbf{v}$ is the velocity of the oscillators given by $\mathbf{v} = (\dot{\phi} \sin \tilde{\theta}, \dot{\tilde{\theta}})$. Substituting for $\mathbf{v}$ using Eqs. (9) gives an evolution equation of

$$0 = \frac{\partial \rho}{\partial t} + \frac{\partial}{\partial \phi} \left\{ \rho \left((\omega + \xi) - \xi \frac{\tan(\tilde{\theta}_F)}{\tan(\tilde{\theta})} R \cos(\phi - \psi) \right) \right\}$$
$$+ \frac{\partial}{\partial \tilde{\theta}} \{ \rho [-\xi \tan(\tilde{\theta}_F) R \sin(\phi - \psi)] \}. \qquad (32)$$

Here the order parameter can be represented in the density formulation as

$$Re^{i\psi} = \int d\omega g(\omega) \int_0^\pi d\tilde{\theta} \sin(\tilde{\theta}) \int_0^{2\pi} d\phi \rho \frac{\sin(\tilde{\theta})}{\sin(\tilde{\theta}_F)} e^{i\phi}. \qquad (33)$$

Interactions between neutrinos occurs through the order parameter.

A. Perturbations about an incoherent state

We wish to describe the evolution of the density function in the neighborhood of an incoherent solution. For neutrinos oscillating in vacuum, the incoherent state corresponds to neutrinos uniformly distributed around the cone in Fig. 1. We shall use this here as our initial zeroth order state.

$$\rho_0(\tilde{\theta}, \phi, \omega, t) = \frac{\delta(\tilde{\theta} - \tilde{\theta}_F)}{2\pi \sin(\tilde{\theta}_F)}. \qquad (34)$$

The denominator is chosen to insure that ρ_0 satisfies the normalization, Eq. (30). Substituting this into the expression for the order parameter, Eq. (33), we see that $R = 0$ for this incoherent state. Consequently, the nonlinear terms in the evolution equation, Eq. (32), vanish and it is straightforward to verify that the incoherent vacuum solution, Eq. (34), is also a solution of the nonlinear evolution equation.

Now we consider small perturbations about the incoherent state.

$$\rho = \rho_0(\tilde{\theta}, \phi, \omega, t) + \epsilon \eta(\tilde{\theta}, \phi, \omega, t) \qquad (35)$$

where $\epsilon \ll 1$. Note that Eq. (30) determines the normalization condition for η as

$$\int_0^\pi d\tilde{\theta}\,\sin\,\tilde{\theta}\int_0^{2\pi}d\phi\,\eta(\tilde{\theta},\phi,\omega,t)=0. \qquad (36)$$

The function η is a deviation from the incoherent state, so it induces an order parameter the size of the perturbation, ϵ.

$$Re^{i\psi}=\epsilon R_1 e^{i\psi}$$

$$=\epsilon\int d\omega g(\omega)\int_0^\pi d\tilde{\theta}\,\sin\,\tilde{\theta}\int_0^{2\pi}d\phi\,\eta\,\frac{\sin(\tilde{\theta})}{\sin(\tilde{\theta}_F)}e^{i\phi}. \qquad (37)$$

Then the evolution equation at order ϵ is

$$0=\frac{\partial\eta}{\partial t}+(\omega+\xi)\frac{\partial\eta}{\partial\phi}+\rho_0\xi R_1\sin(\phi-\psi)$$

$$-\xi\,\tan(\tilde{\theta}_F)R_1\sin(\phi-\psi)\,\frac{\partial\rho_0}{\partial\tilde{\theta}}. \qquad (38)$$

This linear equation describes the growth of the order parameter near the incoherent state.

Our goal is to determine the behavior of the order parameter as a function of time. It is instructive to note from Eq. (37) that the factor multiplying the density function in the definition of the order parameter is proportional to a spherical harmonic:

$$\sin(\tilde{\theta})e^{i\phi}=-\sqrt{\frac{8\pi}{3}}\,Y_{1,1}(\tilde{\theta},\phi)=\sqrt{\frac{8\pi}{3}}\,Y_{1,-1}^*(\tilde{\theta},\phi). \qquad (39)$$

Thus, because the spherical harmonics are orthogonal, only the part of η that is proportional to $Y_{1,-1}$ contributes to the order parameter. Hence, it makes sense to expand η in spherical harmonics.

$$\eta(\tilde{\theta},\phi,\omega,t)=\sum_{l=1}^\infty\sum_{m=-l}^l A_{l,m}(\omega,t)Y_{l,m}(\tilde{\theta},\phi). \qquad (40)$$

The coefficients $A_{l,m}$ are the amplitudes of the different modes of oscillation. The normalization condition requires $A_{0,0}=0$ and because η is real, $A_{l,m}=(-1)^m A_{l,-m}^*$. The order parameter is

$$R_1 e^{i\psi}=\frac{1}{\sin(\tilde{\theta}_F)}\sqrt{\frac{8\pi}{3}}\int d\omega g(\omega)A_{1,-1}(\omega,t). \qquad (41)$$

To pick out the $A_{1,-1}(\omega,t)$ amplitude from the linearized evolution equation, we multiply Eq. (38) by $Y_{1,-1}^*(\tilde{\theta},\phi)$ and then integrate over $\tilde{\theta}$ and ϕ. This gives

$$0=\frac{\partial A_{1,-1}(\omega,t)}{\partial t}-i(\omega+\xi)A_{1,-1}(\omega,t)$$

$$+i\frac{3\xi}{2}\int d\omega g(\omega)A_{1,-1}(\omega,t). \qquad (42)$$

This simple amplitude equation determines the growth of the order parameter. The analogous amplitude equation derived for the Kuramoto model is almost identical to this, the only difference being the coefficient of the integral is then real. This is rather surprising considering that the neutrino model depends not just on the a phase parameter, but also on the mixing angle parameter. However the final amplitude equation is independent of $\cos(\theta_F)$, except through the ξ parameter. Similar amplitude equations can be easily derived for the other harmonics, however, they are not relevant to the growth of the order parameter.

The equation for the $A_{1,-1}$ amplitude, Eq. (42), has a discrete and a continuous spectrum of eigenvalues [28]. This is not surprisingly, since the numerical solution found localized and continuous structure. The continuous spectrum is responsible for phase mixing which causes the order parameter to decrease in time. The discrete solution is responsible for the steady state behavior of the order parameter. The equation can be solved completely, to find the relative amplitudes of the discrete and continuous solutions, using Laplace transforms (see the Appendix). Here we shall confine our analysis to the physically most interesting part, the discrete eigenvalue. It is of the form

$$A_{1,-1}(\omega,t)=B(\omega)e^{\lambda t} \qquad (43)$$

where the eigenvalue is independent of ω. Substituting this in yields an equation for the eigenvalue λ of

$$\lambda B=i(\omega+\xi)B-i\frac{3\xi}{2}\int dfg(f)B(f). \qquad (44)$$

This equation is easy to solve because the integral is just a constant, independent of ω. Let the value of this constant be denoted by C. Then we can solve for $B(\omega)$

$$B(\omega)=-i\left(\frac{3\xi}{2}\right)\frac{C}{\lambda-i(\omega+\xi)}. \qquad (45)$$

Substituting this back into the equation for the eigenvalue, Eq. (44), the constant C cancels out, since C must be nonzero, otherwise, the solution is trivial. Then the equation for the eigenvalue is

$$1=\frac{3\xi}{2}\int d\omega\,\frac{g(\omega)}{(\omega+\xi)+i\lambda} \qquad (46)$$

where we have canceled out a factor of i from the numerator and denominator [compare to Eq. (20)]. This equation specifies the time dependence of the synchronized state.

The eigenvalue equation can be solved analytically for specific frequency distribution functions, $g(\omega)$. However even without solving it, we can deduce an important property

about the eigenvalue. Writing $i\lambda = x + iy$, the imaginary part of this eigenvalue equation can be written as

$$0 = y \frac{3\xi}{2} \int d\omega \frac{g(\omega)}{(\omega + \xi + x)^2 + y^2}. \tag{47}$$

The integral in this equation is necessarily nonzero because all physical $g(\omega)$ are positive at every frequency, and because the denominator is always positive. Thus for nonzero ξ, the last equation shows that $y = 0$. Consequently, the eigenvalue must always be purely imaginary. In the Kuramoto model, the eigenvalue has a real part with leads to exponential growth of the order parameter. But the results here clearly indicate that for the neutrino dynamics model, the incoherent state has neutral stability, and the magnitude of the order parameter will never increase or decrease exponentially in time.

1. Solution for uniform spectrum

The integration in Eq. (46) can be performed for a uniform frequency distribution, Eq. (21). Then, solving for λ yields

$$\lambda = i \left[\xi - \gamma \coth\left(\frac{2\gamma}{3\xi} \right) \right]. \tag{48}$$

Using this result, we see that the integrand in Eq. (46) is never singular, since $(i\lambda + \xi) > \gamma$ for all nonzero values of ξ. Only for $\xi = 0$ does the denominator of the integral vanish, indicating that the discrete solution disappear. Thus in the neutrino model, a steady state synchronized solution exists for all values of the nonlinear coupling, ξ.

This result is used to generate the theoretical curve plotted on Fig. 3(b). The phase of the order parameter is related to the eigenvalue by Eqs. (41) and (43), which gives $(d\psi/dt - \xi) = (-i\lambda - \xi)$. In the figure, the theoretical prediction agrees well with the numerical results when ξ is small. At large ξ the order parameter is large and our linearized method breaks down.

2. Solution for delta function spectrum

The previous frequency distribution is an even, single humped function. These are rather special properties and frequency distributions without them may have qualitatively different behavior [33]. For generality, we examine a frequency distribution which does not have these properties. In particular, consider the sum of two delta functions, centered at frequencies ω_α and ω_β.

$$g(\omega) = \alpha \delta(\omega - \omega_\alpha) + (1 - \alpha) \delta(\omega - \omega_\beta). \tag{49}$$

Here α parameterizes the relative amount of each frequency, while keeping the overall normalization of $g(\omega)$ equal to 1. Since $g(\omega)$ must always be positive, the parameter α is restricted to the range $0 \leq \alpha \leq 1$. This bimodal distribution is not an even function of frequency, except at $\alpha = 0.5$.

The integration of Eq. (46) can be easily performed for a delta function integrand. Then, solving for λ yields

$$\lambda = i\xi + i \frac{1}{2} \left\{ \left[\omega_\beta + \omega_\alpha - \frac{3\xi}{2} \right] \pm \left[\left(\omega_\beta - \omega_\alpha - \frac{3\xi}{2}(1 - 2\alpha) \right)^2 \right. \right.$$
$$\left. \left. + (3\xi)^2 \alpha(1 - \alpha) \right]^{1/2} \right\}. \tag{50}$$

There are now two eigenvalues. In the limit that $\xi \to 0$, the roots just reduce to the vacuum frequencies, ω_α and ω_β. In the limit of $\alpha \to 0$ or 1, only one of the delta functions is relevant and the two roots are then just the vacuum frequency of the decoupled oscillator, and the other vacuum frequency minus $3\xi/2$. The most important feature is that, for all values of ξ and for any physical value of α, the argument of the square root is positive. Thus, the discrete eigenvalue is always purely imaginary, in agreement with the arguments from Eq. (47). The incoherent state has neutral stability.

B. Perturbations about two mixing angles

The previous analytical calculations assumed the neutrinos were predominantly incoherent in phase with a single mixing angle. However it is more physical to consider a zeroth order state which has a distribution of mixing angles. Such distributions can be produced by nonlinear effects [see, e.g., Fig. 4(c)], or they can also be produced by effects not included in the present neutrino dynamics model, such as MSW type effects. To search for any qualitatively new features associated with such a state, we consider perturbations about a generalization of Eq. (34).

$$\rho_0(\tilde{\theta}, \phi, \omega, t) = Q(\omega) \frac{\delta(\tilde{\theta} - \tilde{\theta}_1)}{2\pi \sin(\tilde{\theta}_1)}$$

$$+ [1 - Q(\omega)] \frac{\delta(\tilde{\theta} - \tilde{\theta}_2)}{2\pi \sin(\tilde{\theta}_2)}. \tag{51}$$

This density function describes neutrinos uniformly distributed in phase at two discrete mixing angles. Here $Q(\omega)$ parameterizes the relative amount of each mixing angle as a function of frequency, while the overall normalization satisfies Eq. (30). Because the density function must be nonnegative, Q is limited to the range $0 \leq Q \leq 1$. The average mixing angle, $\tilde{\theta}_F$, is determined by

$$\cos(\tilde{\theta}_F) = \int d\omega g(\omega)[Q(\omega)\cos(\tilde{\theta}_1) + [1 - Q(\omega)]\cos(\tilde{\theta}_2)] \tag{52}$$

and θ_F lies between the two mixing angles, $\tilde{\theta}_1$ and $\tilde{\theta}_2$. Because the phase is uniformly distributed, the order parameter vanishes and so this density solves the nonlinear evolution equation, Eq. (31).

Starting from this zeroth order state, the calculation can proceed parallel to the one outlined in Sec. IV A. The perturbations can be written as an expansion in spherical harmonics. Then the equations describing the evolution of the amplitudes can be derived. Again the $A_{1,-1}$ amplitude is the only one responsible for the growth of the order parameter, and it has a discrete solution. The eigenvalue equation for this solution is

$$1 = \frac{3\xi}{2} \int d\omega \, \frac{g(\omega)q(\omega)}{(\omega + \xi) + i\lambda}. \tag{53}$$

The only difference between this eigenvalue equation and that derived previously for a single mixing angle, Eq. (46), is the additional function in the integrand, $q(\omega)$, defined as

$$q(\omega) = \left(\frac{2}{3} + \frac{\{Q(\omega)\sin(\tilde{\theta}_1) + [1 - Q(\omega)]\sin(\tilde{\theta}_2)\}}{3\,\sin(\tilde{\theta}_F)} \right). \tag{54}$$

Because $0 \le \tilde{\theta} \le \pi$ and $0 \le Q \le 1$, $q(\omega)$ is necessarily nonnegative for all frequencies. Thus the effects of introducing $q(\omega)$ into the eigenvalue equation can be absorbed into the frequency distribution, $g(\omega)$, and the nonlinear constant, ξ. That is, the eigenvalues derived from this "two mixing angle" equation are not qualitatively different than those derived from the previous "one mixing angle" eigenvalue equation. In particular, the proof that the eigenvalues are necessarily purely imaginary, Eq. (47), holds for this new eigenvalue equation. The incoherent state in Eq. (51) has neutral stability.

V. CONCLUSIONS

In this paper we have analyzed the flavor dynamics of a dilute, isotropic gas of massive neutrinos. The only interaction included was the neutrino-neutrino forward scattering, which is a large and often dominant effect in the early universe, and which is also relevant in type II supernovae. This interaction makes the flavor evolution nonlinear and thus collective phenomena can be important.

The dynamics were described using a phase and mixing angle formalism. This parametrization is efficient, intuitive, and allows us to adopt methods from the extensive literature on the synchronization of oscillators. Writing the equations of motion in this parametrization immediately suggests a specific order parameter for the system. Also, it is apparent that synchronization of phases leads to evolution of the mixing angle. The behavior of the neutrino system, and in particular, the order parameter, was studied numerically and analytically.

Numerical simulations provided useful examples of the behavior in this nonlinear dynamical system, Figs. 2–4. However numerical simulations have their limitations and these were also examined. Numerical simulations necessarily require a discrete number of "neutrinos" to evolve, and this number is far less than the number of neutrinos present in physical systems. This places a severe limit on the length of time for which numerical simulations will accurately model the physical system [see Eq. (24)]. As time increases, the neutrino spectrum is probed at decreasing frequency scales, so increasing numbers of neutrinos are needed to model this accurately. This effect has been ignored in previously published numerical studies of nonlinear neutrino systems, consequently, those previous results must be used with caution.

Our numerical and analytical analyses show that the incoherent state has neutral stability. Neutrino systems that are initially incoherent, remain incoherent, while systems that are initially synchronized remain synchronized. However the amount of synchronization supportable by the system depends on the width of the neutrino spectrum, and on the number of neutrinos per unit volume. At large neutrino number densities, the system can be completely synchronized. At small neutrino number densities, some of the synchronization can decay via phase mixing, but a small amount of synchronization is always supportable.

The amount of synchronization possible in our neutrino system was determined analytically by defining a continuous density function to describe the distribution of oscillators. This formalism is extremely powerful and allowed us to study the behavior of the system near the incoherent state. Using this technique, an approximate expression for the steady state value of the order parameter's magnitude and phase was derived [Eq. (A9)]. This analytical expression agreed well with the numerical simulations (Fig. 3).

The neutrino system studied in this paper is too simple to make definite predictions about the physical environments, where neutrino-neutrino forward scattering is relevant. In the early universe and in type II supernovae, there are always the additional effects of antineutrino degrees of freedom and of three neutrino flavors. At various times, there are other effects which are relevant: forward scattering off of charged leptons, nonforward scattering, spatial anisotropy, and density fluctuations. All of these possibilities can be studied with the techniques used in this paper. Work on them is in progress. However we shall briefly speculate on how these effects modify the results found here.

The "steady state" of the neutrino model studied here depends on the initial amount of synchronization. This is because this model is approximately a conservative system [see Eq. (28)]. The addition of antineutrino degrees of freedom to the system is not likely to change this. Similarly, the addition of a constant electron background is not expected to make the system dissipative. However if the electron background is allowed to vary with time, this would qualitatively change the situation. For example, an electron background density that decreased monotonically in time might induce synchronization—since it does so when the neutrino background is negligible and the MSW transition is nonadiabatic. The neutrino-neutrino forward scattering might then sustain the synchronization after the electron background became negligible. But if the electron background density fluctuated randomly, then this would most likely make the incoherent state stable. Calculations in the Kuramoto model have shown that random fluctuations tend to make the incoherent state stable. However the Kuramoto model also illustrates how dissipative effects can cause the generation of synchronization by making the incoherent state unstable. The similarity of the neutrino model to the Kuramoto model, Eq. (18), makes it seem likely that the incoherent state may be unstable in some neutrino systems. In particular, it is easy to show that only a small phase shift needs to be added to the neutrino model's cosine coupling to make the incoherent state unstable. Such a phase shift might come from the T violating phase that is intrinsic with three neutrino flavors. Nonforward scattering and spatial anisotropy might also have a similar effect. It appears possible that collective flavor

phenomena are a robust feature of some high density neutrino systems.

APPENDIX: CALCULATING THE STEADY STATE ORDER PARAMETER

The linear amplitude equation, Eq. (42), can be solved completely using Laplace transformations [30]. Here we use this to calculate the steady state value of the order parameter.

Multiplying through Eq. (42) by e^{-st} and integrating over t yields

$$[s-i(\omega+\xi)]\tilde{A}(\omega,s)=A(\omega,0)-i\left(\frac{3\xi}{2}\right)\int d\omega g(\omega)\tilde{A}(\omega,s)$$

$$(A1)$$

where the Laplace transform of A is

$$\tilde{A}(\omega,s)=\int_0^\infty dt e^{-st}A(\omega,t) \qquad (A2)$$

and the $(1,-1)$ subscripts on A have been dropped. The order parameter depends on the integral of A over frequency as given in Eq. (41). Thus we calculate the integral of the Laplace transform of A over frequency. Using Eq. (A1) yields

$$\int d\omega g(\omega)\tilde{A}(\omega,s)=\frac{\int d\omega g(\omega)A(\omega,0)/[s-i(\omega+\xi)]}{1+i(3\xi/2)\int d\omega g(\omega)/[s-i(\omega+\xi)]}. \qquad (A3)$$

Then the order parameter is given by

$$R_1 e^{i\psi}=C\int_{a-i\infty}^{a+i\infty} ds e^{st}\int d\omega g(\omega)\tilde{A}(\omega,s) \qquad (A4)$$

where the contour of integration lies to the right of all singularities. C is an unimportant constant that can be absorbed into $A(\omega,0)$.

We wish to consider the case, where the neutrinos are initially synchronized. Then $A(\omega,0)$ is the same for all neutrinos so it is a constant, independent of frequency. We further restrict the calculation to a uniform frequency distribution, as described in Eq. (21). Then the integrations over frequency can be easily performed to yield

$$R_1 e^{i\psi}=C'\int_{a-i\infty}^{a+i\infty} ds e^{st}$$

$$\times \frac{\ln[(\gamma+\xi+is)/(-\gamma+\xi+is)]}{1-(3\xi/4\gamma)\ln[(\gamma+\xi+is)/(-\gamma+\xi+is)]}.$$

$$(A5)$$

In the complex s plane, the integrand has a pole and two branch points, all on the imaginary axis. The pole is determined by setting the denominator equal to zero, which yields an equation identical to Eq. (46). The pole location is thus given by Eq. (48), with $s_0=\lambda$, thus the pole lies below both branch points (for $\xi>0$). Consequently, we choose both branch cuts to lie on the imaginary axis above the branch points, so that in the integrand, the two branch cuts cancel out above the upper branch point. Then the integration contour can be deformed, so the integral has two pieces, the pole term and the integration around the branch cut connecting the two branch points.

The pole part of the integrand is straightforward to calculate, it is

$$[R_1 e^{i\psi}]_{\text{pole}}=C'(4\pi\gamma)\frac{(2\gamma/3\xi)^2}{\sinh^2(2\gamma/3\xi)}e^{s_0 t}. \qquad (A6)$$

To get the normalization constant, we need to know the total integral at $t=0$. At $t=0$, the integration between the branch points can be rewritten as

$$[R_1 e^{i\psi}]_{\text{continuous}}|_0=C'(2\pi\gamma)\int_{-1}^1 dy\left\{\left[1-\left(\frac{3\xi}{4\gamma}\right)\ln\left(\frac{1-y}{1+y}\right)\right]^2\right.$$

$$\left.+\left(\frac{\pi3\xi}{4\gamma}\right)^2\right\}^{-1}. \qquad (A7)$$

An exact, analytical expression for the last integral could not be found, however, a good approximate expression is easy to obtain. Because the logarithm is slowly varying, and because it vanishes in the middle of the integration region at $y=0$, it is an extremely good approximation to just neglect it in the integrand:

$$[R_1 e^{i\psi}]_{\text{continuous}}|_0\simeq C'(4\pi\gamma)\frac{1}{1+(\pi3\xi/4\gamma)^2}. \qquad (A8)$$

Using this and the expression for the pole term yields an expression for the steady state value of the order parameter:

$$R_1 e^{i\psi}|_{\text{steady state}}\simeq\left[1+\frac{(3\xi/2\gamma)^2 \sinh^2(2\gamma/3\xi)}{1+(\pi3\xi/4\gamma)^2}\right]^{-1}e^{s_0 t}. \qquad (A9)$$

The magnitude of this equation is plotted in Fig. 3(a), where it is compared to the results of numerical simulations. There is good agreement, considering that this analytical expression is derived from the linearized evolution equation. The phase of the steady state order parameter is just the phase of the pole term, and it agrees with the calculation in Sec. IV A 1. The phase is plotted in Fig. 3(b) and agrees with the numerical results when the magnitude of the order parameter is small.

[1] J. N. Bahcall, M. H. Pinsonneault, S. Basu, and J. Christensen-Dalsgaard, Phys. Rev. Lett. **78**, 171 (1997); J. N. Bahcall and M. H. Pinsonneault, Rev. Mod. Phys. **67**, 781 (1995).

[2] R. Davis, D. S. Harmer, and K. C. Hoffman, Phys. Rev. Lett. **20**, 1205 (1968); K. Lande, in *Proceedings of the Neutrino 96*, edited by K. Enqvist, K. Huitu, and J. Maalampi (World Scientific, Singapore, 1996), p. 25; Kamiokande Collaboration, Y. Fukuda *et al.*, Phys. Rev. Lett. **77**, 1683 (1996); GALLEX Collaboration, W. Hampel *et al.*, Phys. Lett. B **388**, 384 (1996); SAGE Collaboration, J. N. Abdurashitov *et al.*, *ibid.* **328**, 234 (1994); Superkamiokande Collaboration, K. Young *et al.*, in http://www.phys.washington.edu/young/superk/drafts/aps97.html

[3] Kamiokande Collaboration, K. S. Hirata *et al.*, Phys. Lett. B **280**, 146 (1992); IMB Collaboration, R. Becker-Szendy *et al.*, Phys. Rev. D **46**, 3720 (1992); Frejus Collaboration, Ch. Berger *et al.*, Phys. Lett. B **245**, 305 (1990); Soudan2 Collaboration, W. W. M. Allison *et al.*, *ibid.* **391**, 491 (1997).

[4] Super-Kamiokande Collaboration, Y. Totsuka *et al.*, Talk at the Lepton-Photon '97, Hamburg, Germany, 1997; Kamiokande Collaboration, Y. Fukuda *et al.*, Phys. Lett. B **335**, 237 (1994).

[5] LSND Collaboration, C. Athanassopoulos *et al.*, Phys. Rev. Lett. **77**, 3082 (1996).

[6] See, e.g., G. Borner, *The Early Universe* (Springer-Verlag, Berlin, 1988); S. Weinberg, *Gravitation and Cosmology* (Wiley, New York, 1972).

[7] S. Weinberg, Phys. Rev. Lett. **43**, 1566 (1979); M. Gell-Mann, P. Ramond, and R. Slansky, *Supergravity*, edited by P. van Nieuwenhuizen and D. Z. Freedman (North-Holland, Amsterdam, 1979), p. 315; T. Yanagida, Proceedings of the Workshop on Unified Theory and Baryon Number of the Universe Tsukuba, Ibaraki, Japan, 1979 (unpublished); R. N. Mohapatra and G. Senjanovic, Phys. Rev. Lett. **44**, 912 (1980).

[8] H. A. Bethe, Phys. Rev. Lett. **56**, 1305 (1986); Fuller *et al.*, Astrophys. J. **322**, 795 (1987).

[9] T. K. Kuo and J. Pantaleone, Rev. Mod. Phys. **61**, 937 (1989).

[10] F. N. Loreti and A. B. Balantekin, Phys. Rev. D **50**, 4762 (1994); F. N. Loreti, Y. Z. Qian, G. M. Fuller, and A. B. Balantekin, *ibid.* **52**, 6664 (1995).

[11] Y. Z. Qian *et al.*, Phys. Rev. Lett. **71**, 1965 (1993).

[12] A. Kusenko and G. Segre, Phys. Rev. Lett. **77**, 4872 (1996).

[13] P. Langacker, S. T. Petcov, G. Steigman, and S. Toshev, Nucl. Phys. **B282**, 589 (1987); M. J. Savage, R. A. Malaney, and G. M. Fuller, Astrophys. J. **368**, 1 (1991); K. Enqvist, K. Kainulainen, and J. Maalampi, Nucl. Phys. **B349**, 754 (1991).

[14] J. Liu and G. Segre, Phys. Lett. B **338**, 259 (1994); A. Casas, W.-Y. Cheng, and G. Gelmini, hep-ph/9709289; A. D. Dolgov and B. E. J. Pagel, astro-ph/9711202.

[15] L. Wolfenstein, Phys. Rev. D **17**, 2369 (1978); **20**, 2634 (1979); S. P. Mikheyev and A. Yu Smirnov, Yad. Fiz. **42**, 1441 (1985) [Sov. J. Nucl. Phys. **42**, 913 (1985)]; Nuovo Cimento C **9**, 17 (1986).

[16] S. P. Mikheyev and A. Yu Smirnov, Usp. Fiz. Nauk **153**, 3 (1987) [Sov. Phys. Usp. **30**, 759 (1987)].

[17] J. Pantaleone, Phys. Lett. B **287**, 128 (1992); J. Pantaleone, Phys. Rev. D **46**, 510 (1992).

[18] A. D. Dolgov, Sov. J. Nucl. Phys. **33**, 700 (1981); L. Stodolsky, Phys. Rev. D **36**, 2273 (1987); M. J. Thomson and B. McKellar, Phys. Lett. B **259**, 113 (1991).

[19] S. Samuel, Phys. Rev. D **48**, 1462 (1993).

[20] G. Sigl and G. Raffelt, Nucl. Phys. **B406**, 423 (1993).

[21] J. Pantaleone, Phys. Lett. B **342**, 250 (1995).

[22] G. Sigl, Phys. Rev. D **51**, 4035 (1995).

[23] V. A. Kostelecky, J. Pantaleone, and S. Samuel, Phys. Lett. B **315**, 46 (1993).

[24] V. A. Kostelecky and S. Samuel, Phys. Rev. D **49**, 1740 (1994); **52**, 3184 (1995); Phys. Lett. B **318**, 127 (1993); **385**, 159 (1996).

[25] V. A. Kostelecky and S. Samuel, Phys. Rev. D **52**, 621 (1995); S. Samuel, *ibid.* **53**, 5382 (1996).

[26] Y. Kuramota, in *International Symposium on Mathematical Problems in Theoretical Physics*, edited by H. Araki (Springer, New York, 1975); Y. Kuramoto, *Chemical Oscillations, Waves and Turbulence* (Springer, Berlin, 1984).

[27] H. Sakaguchi and Y. Kuramoto, Prog. Theor. Phys. **76**, 576 (1986).

[28] S. H. Strogatz and R. E. Mirollo, J. Stat. Phys. **63**, 613 (1991).

[29] P. C. Matthews and S. H. Strogatz, Phys. Rev. Lett. **65**, 1701 (1990); P. C. Matthews, R. E. Mirollo, and S. H. Strogatz, Physica D **52**, 293 (1991).

[30] S. H. Strogatz, R. E. Mirollo, and P. C. Matthews, Phys. Rev. Lett. **68**, 2730 (1992).

[31] J. L. van Hemmen and W. F. Wreszinski, J. Stat. Phys. **72**, 145 (1993).

[32] L. L. Bonnilla, C. J. Perez Vicente, and J. M. Rubi, J. Stat. Phys. **70**, 921 (1993).

[33] J. D. Crawford, J. Stat. Phys. **74**, 1047 (1994).

[34] D. C. Michaels, E. P. Matyas, and J. Jalife, Circ. Res. **61**, 704 (1987); J. Buck, Q. Rev. Biol. **63**, 265 (1988); T. J. Walker, Science **166**, 891 (1969).

[35] S. H. Strogatz, C. M. Marcus, R. M. Westervelt, and R. E. Mirollo, Physica D **36**, 23 (1989).

[36] D. Nötzold and G. Raffelt, Nucl. Phys. **B307**, 924 (1988); G. M. Fuller, R. W. Mayle, J. R. Wilson, and D. N. Schramm, Astrophys. J. **322**, 795 (1987).

[37] S. H. Strogatz and I. Stewart, Sci. Am. Dec., p. 102 (1993).